Dermis mechanical behaviour after different cell removal treatments

Dermis Mechanical Behaviour after Different Cell Removal Treatments

Mara Terzini[a], Cristina Bignardi[b], Carlotta Castagnoli[c], Irene Cambieri[d], Elisabetta M. Zanetti[e]*, Alberto L. Audenino[f]

[a]DIMEAS, Politecnico di Torino, Cso Duca degli Abruzzi, 10129 Torino (ITALY); E-mail: mara.terzini@polito.it

[b]DIMEAS, Politecnico di Torino, Cso Duca degli Abruzzi, 10129 Torino (ITALY); E-mail: cristina.bignardi@polito.it

[c]Skin Bank, AOU Città della Salute e della Scienza, Via Zuretti 29, 10126 Torino (ITALY); E-mail: ccastagnoli@cittadellasalute.to.it

[d]Skin Bank, AOU Città della Salute e della Scienza, Via Zuretti 29, 10126 Torino (ITALY); E-mail: icambieri@cittadellasalute.to.it

[e]DI, University of Perugia, Via Duranti 67, 06125 Perugia (ITALY); E-mail: elisabetta.zanetti@unipg.it

[f]DIMEAS, Politecnico di Torino, Cso Duca degli Abruzzi, 10129 Torino (ITALY); E-mail: alberto.audenino@polito.it

Running Head: Dermis Mechanical Behavior for Different Cell Removal Treatments

*Contact Author:
Elisabetta M. Zanetti
Department of Engineering
Via Duranti, 67
06125 Perugia (ITALY)
E-mail: elisabetta.zanetti@unipg.it

Abstract

Human acellular dermal matrices (HADMs) are used in reconstructive surgery as scaffolds promoting autologous tissue regeneration. Critical to the HADM ability to remodel and integrate into the host tissue is the removal of cells while maintaining an intact extracellular architecture.

The objective of this work is to develop a methodology to analyse the mechanical properties of HADMs after decellularization to identify its ideal form of treatment and its duration.

Two different decellularization techniques were used as a benchmark: the first is a well-established technique (incubation in NaOH for 1 to 7 weeks), and the second is an innovative technique developed by this research group (incubation in DMEM (Dulbecco's modified Eagle medium) for 1 to 7 weeks). After decellularization, the specimens underwent uniaxial tensile tests, and experimental data were represented with stress strain curves, calculating both engineering and true values.

Mechanical tests have led to the identification of the optimal method (NaOH or DMEM) and duration for the decellularization treatment; differences between engineering and true values can reach 84%, but the engineering values remain useful to make comparisons, providing reliable indications with a simpler experimental set up and data processing.

Keywords – decellularization treatment, human dermis, static mechanical tests, ultimate stress, ultimate strain, Young’s modulus

1 Introduction

Engineered skin substitutes have a significant medical practice for patients with extensive burn wounds [1]. Advances in tissue engineering suggest that skin substitutes will be indistinguishable from the normal skin in the near future [2]. However, current skin substitutes do not restore the full native skin physiology because they lack some components such as hair follicles, sebaceous glands and sweat glands [2]. Additionally, the engineered tissue cannot faithfully replicate the mechanical properties of the native skin [1].

Currently, alloplastic material and skin allografts, taken from multi-organ donors, are the most suitable integumentary replacement for reconstructive surgery [3]. The immune response to allograft skin is directed primarily against epidermal, endothelial and fibroblast cells in the dermis, while the non-cellular component of the dermis (extracellular matrix) has been demonstrated to be relatively non-immunogenic [4]. Glycerolised acellular alloplastic human dermis (HADM) is used as a matrix for various reconstructive plastic purposes, where it retains almost all of the healthy dermal properties: it is compact and elastic, can be taken into the bed wound, and it retains the intact tissue morphology [5].

Different treatments can be used for tissue decellularization [6]. Commonly, a low concentration of NaOH has been used for this aim. The result of this technique is a reliably decellularized matrix. However, surgeons report that this matrix is inferior with reference to handling, ease of use, elasticity and needle penetration resistance. Additionally, decellularization using sodium hydroxide implies the direct contact of the tissue with an aggressive chemical agent, which must necessarily be neutralized by means of incubation in 0.1 N HCl at the end of the decellularization phase. These are the reasons why, in recent times, our research unit has developed an alternative procedure that aims to overcome these limitations. The new methodology consists of keeping the

tissue in DMEM (Dulbecco's modified Eagle medium) for a long period of time (several weeks) while being subjected to mechanical action (tilting). From a biological point of view, the efficiency of the different treatments can be verified by means of an immunohistochemistry analysis, but the preservation of the main mechanical properties of the native dermis also needs to be checked [7]. The aim of this work is to evaluate the mechanical properties of tissue subjected to decellularization treatments varying by type and length to establish the best compromise between a reliably complete decellularization and adequate mechanical properties. The mechanical properties here analysed are the elastic modulus and the ultimate load and strain [8], considering that repaired full-thickness burn wounds may be subject to loss due to dermal substitute deficiencies in tensile strength and elasticity [1] and the requirements of soft-tissue augmentation procedures like rotator cuff [9].

The skin is made of three layers, the epidermis, dermis, and hypodermis. It consists of collagen (approximately 75% of the dry weight) and elastin (4% of the dry weight) fibres embedded in a gel-like ground substance consisting of water, small solutes, and macromolecules, predominantly proteoglycans [10]. The dermis provides a major contribution to the overall mechanical characteristics of the skin due to its main constituents, collagen and elastin fibrils, which allow high levels of deformation and flexibility as the fibrils stretch and re-orientate [11]. Collagen fibres are crimped and almost inactive at low strains, while they play a major role at high deformations (where they are stiffer than elastin by approximately three order of magnitude [8]). The skin is anisotropic due to the variable orientation of collagen fibres, with a prevalence along the orientation of the so-called Langer’s lines [8]. The dermis can therefore be described as an anisotropic, viscoelastic, nonlinear [12] and non-homogenous material.

The tensile test is the most widely used mechanical test performed on *ex vivo* skin specimens. Using this method, the anisotropic, non-linear and viscoelastic behaviours of skin have been explored, as well as its failure properties [13], creep [14], fatigue [15] and preconditioning behaviour [16]. This test is here being used to assess changes in the biomechanical behaviour produced by alterations of the skin's structure, similarly to the approach followed by those authors who studied variations in the collagen content [14] or elastin and proteoglycans contents [10].

Due to section narrowing taking place during the specimen loading, different formulations of stress in mechanical tests can produce different results: these are the so called 'nominal' or 'engineering values'; their respective 'true' values can be obtained from engineering values under specific assumptions such as volume constancy [17,18]. As true values provide the most faithful representation of the material properties, their estimation requires a complex and demanding experimental set up. This work is also an attempt to quantify differences among these expressions and their limits, establishing if they can or cannot be used for tissue characterization and/or to make comparisons among decellularization treatments.

2 Materials and methods

2.1 Specimens

Strips of skin tissue, collected from the backs of human donors, were dissected along the cranio-caudal direction. They were decellularized using two different methods based on incubation in 0.06 N NaOH or DMEM for 1 to 7 weeks. Immunohistochemistry has been performed for all treatments to verify the decellularization, according to the following procedure. Biopsy samples were washed in physiological solution, fixed in 4% neutral-buffered formalin and embedded in formalin by routine processing (FFPE). FFPE samples were sectioned at a thickness of 2-3 μm

for immunohistochemistry reactions, and immunohistochemistry was performed using an automated slide-processing platform (Ventana BenchMarckXT Autostainer, Ventana Medical Systems, Tucson, AZ, USA).” HADMs, preserved at 85% glycerol in a 4°C refrigerator at the Turin Skin Bank (Italy) and unfit for transplantation, were used for these experiments after the approval of the Institutional Ethical Board of A*zienda Ospedaliera Universitaria Città della Salute e della Scienza* of Turin, Italy, (approved on January 23rd, 2012 with protocol number 0006730), and written informed consent was obtained from all study participants. Before use, the dermis grafts were washed to remove all of the glycerol, dipping them sequentially in three different beakers filled with abundant saline solution 0.9% at +37°C for more than three minutes each, as prescribed by the Euro Skin Bank [19]. The specimens were obtained by cutting out approximately 2x4 mm strips along the cranio-caudal (CC) and medio-lateral (ML) directions using a custom made die cutter; this cutting method avoids generating notches and defects that could bias tests. The resulting specimen sizes were measured by means of photogrammetry before mechanical testing: 4.33±0.57-mm width, 2.21±0.32-mm thickness, 10.10±0.38-mm length (average ± std).

On the whole, there were 3–4 specimens (depending on the original strip size and shape) for each combination of decellularization method (NaOH or DMEM), duration (called ‘Tx’ in the following, where x represents the number of weeks of incubation) and cut orientation (CC or ML), for a total 96 specimens. Intact human skin was used as a control (called ‘T0’ in the following, as it did not undergo any decellularization treatment).

2.2 Photogrammetry set-up

Two different photographic set-ups have been developed to measure the specimens. The first was finalized to measure the specimens’ size at rest and was made of a full-frame digital camera

(Canon EOS 5D Mark II) with an autofocus lens for macro photography (Canon EF 100 mm f/2.8 Macro USM), a camera stand with two light stands, and a tripod. A second set-up was developed to follow tensile tests; it included the previously described digital camera as well as a second digital single-lens reflex camera (Canon EOS 400D). When the two cameras were triggered, they acquired the frontal and lateral views of the specimen through a remote capture software (DSLR Remote Pro). The width and the thickness of the specimens were measured using the image analysis software ImageJ (National Institutes of Health, Bethesda, Maryland, U.S.) as an average of five different measurements, reaching a 0.01 mm/pixel measurement resolution given a 21.0 MP image (5616x3744 pixels).

2.3 Mechanical tests

Samples were subjected to uniaxial tensile tests along both the cranio-caudal and medio-lateral directions to quantify the influence of the chemical treatment on the skin tissue's biomechanical behaviour. Testing parameters have been set according to the physiological loads, the expected tissue behaviour, and the Bose Electroforce® features. For example, the strain rate could reach very high values in reality due to impact forces, but the characteristics of the material are strain rate dependent [20], and the test speed had to be limited to 3.2%/s so as not to exceed the load cell range and risking rupture. The specimen length also had to be chosen considering the physiologic peak strain (over 100%) and the machine stroke (±6 mm), together with the limited sample extension; these considerations led to the selection of a ~~10~~ 5 mm specimen length. The specimens were clamped by titanium machine grips that were specifically developed for biomaterials and have knurled-flat faces to prevent slipping. The analysis of the video recordings demonstrates that there were neither anomalous behaviours nor failures near the clamps. Sliding through the testing grips was excluded, too, as no abrupt increase or decrease was detected in the

163 experimental curves. No marks were observed on the specimen ends, and the extension of the
164 grasped ends was found to be unchanged.
165 Up to the instant preceding the tensile test, all specimens were kept hydrated in physiological
166 solution; no additional hydration was carried out during the test due to the absence of a
167 thermostatic bath. This was not judged to be a major shortcoming because the tests lasted less
168 than one minute. Specimens were constrained to the Bose Electroforce® testing machine,
169 clamping their ends along the longitudinal direction.
170 No preconditioning cycles were performed because the dermal tissue is a bi-phasic structure, like
171 most soft tissues, and preconditioning has been demonstrated to significantly influence the
172 mechanical response of these tissues. Slow viscoelastic phenomena related to fluid flow initiate
173 starting from the very first loading cycles, so the final mechanical properties would depend on the
174 pre-conditioning protocol [21].
175 The testing room temperature was 20° C, while the humidity ranged between 40 and 65%. The
176 displacement was set equal to zero when a 0.05 N force was recorded.
177 Rupture tensile tests were performed for all samples in displacement control at a strain rate of
178 0.032 s^{-1}. The initial gap between the grips was 5 mm.

179 ## 2.4 Data Elaboration

180 The results of rupture tests on soft tissues are often reported in terms of ‘engineering’ stress and
181 strain in the literature, with a few exceptions where the specimen section is monitored during
182 tests, and the strain distribution is assessed by full-field techniques [17,22]. In this work, the
183 engineering and true values have been calculated, as detailed in the following.
184 The "engineering curve" is obtained by ignoring the narrowing of the section during the elongation
185 of the sample and referring always to the initial specimen length. The engineering stress σ_e (Eq.

1) is therefore calculated by dividing the force F by the unloaded-cross sectional area A_0 of the specimen; the engineering strain ε_e (Eq. 2) is expressed as the change in length ΔL per unit of the original length L_0. It should be emphasised that the measurement of the engineering strain would require a dog-bone shaped specimen and a calibrated length whose elongation is monitored, while a rectangular specimen has been here used and its elongation has been evaluated on the basis of the clamp-to-clamp displacement; the authors considered that this was not a hard limitation due to the high compliance of the tissue, which "homogenises" the stress field (see, for example, the work of Taylor et al. on crack propagation [23]). The engineering Young's modulus (E_e) has been calculated from the linear portion of the stress-strain curve [8], which is the so-called 'linear region' where collagen chains are stretched [12,24]: curve data were locally derived with a moving average linear regression, and the constant trend of the derived curve was considered.

The true stress σ_t is the ratio between the force and the minimum section A_{min}; it is approximately coincident with the engineering curve, up to the strain where section narrowing becomes conspicuous. The true curve can be obtained by monitoring the neck area during the tensile test: the history of the section variation $A_{min}(t)$ needs to be acquired, monitoring both the specimen width $b_{min}(t)$ and thickness $s_{min}(t)$ at the neck region. In the literature, an alternative expression for the true stress is often used, which relies on the hypothesis of a null variation of the specimen volume [25]: this expression is simpler to be implemented because it requires only the estimation of the real-time specimen length (like for the engineering curve). The respective value σ_{st} will be called the 'simplified true' stress, and it can be obtained from the engineering curve by analytical transformations ($\sigma_{st}= \sigma_e \cdot (1+ \varepsilon_e)$). The corresponding 'simplified true' elastic modulus E_{st} can be calculated on $\sigma_{st}/\varepsilon_e$ curves.

The evaluation of the true Young's modulus E_t has been performed on the basis of the acquired force and displacement signals and of the specimen shape; given a certain force *F*, the specimen volume can be divided axially into infinitesimal portions *dy* whose section is *A(y,F)*. Therefore, the whole specimen elongation Δs_{ab} in the linear portion of the force/displacement curve (a, b, figure 1) can be expressed as

$$\Delta s_{ab} = \int_{F_a}^{F_b} \int_0^l ds = \int_{F_a}^{F_b} \int_0^l \varepsilon_t \cdot dy = \int_{F_a}^{F_b} \left[\int_0^l \frac{1}{E_t \cdot A(y,F)} dy \right] dF = \frac{1}{E_t} \int_{F_a}^{F_b} \left[\int_0^l \frac{dy}{A(y,F)} \right] dF$$

where the Young's modulus has been considered to be linear (independent of the force level) and constant all over the specimen, as it should be in the above-mentioned 'linear elastic region'. This formula could not be used up to the failure region (to obtain the true ultimate strain, for example). The 'true' Young's modulus can be so derived:

$$E_t = \frac{\int_{F_a}^{F_b} \left[\int_0^l \frac{dy}{A(y,F)} \right] dF}{\Delta s_{ab}}$$

The numerator requires the knowledge of the section variation for each force step, and at different quotes (*y*), and it can be estimated thanks to the photogrammetry set up.

A number of descriptive parameters can be so obtained: the ultimate tensile strength (UTS, UTS_t, UTS_{st}), the ultimate deformation ($\varepsilon_{UTS,e}$), and the Young's modulus (E_e, E_{st}, E_t). True values have been calculated only for those decellularization treatments that produced 'engineering' and 'simplified true' mechanical properties similar to those of the native dermis ($p<0.05$, Tukey-Kramer test, as detailed in the following).

2.5 Statistical analysis

The mechanical properties of the dermis were reported in relation to the testing direction (CC or ML), the type of decellularization treatment (called NaOH or DMEM in the following), and the

duration of the treatments (from 0 to 7 weeks at 1 week steps, called T0, T1 …. T7 in the following).

The statistical analysis of the experimental results was carried out using a multivariate analysis of variance (Matlab function 'anovan'), followed by a Tukey–Kramer post hoc test, after having tested the normality of the statistical distribution of all parameters by the Lilliefors test function. Significance levels were set to $p < 0.05$ for all tests.

3 Results

The analysis of video recordings demonstrated that there were neither anomalous behaviours nor failures near clamps; therefore, all acquired data have been elaborated.

Figures 2 shows typical stress/strain curves for the engineering, simplified true and true formulations. Dealing with the ultimate stress (Fig. 3-5), the engineering stress leads to underestimate the UTS by up to -71% and the Young's modulus by up to -84%. The simplified true stress would underestimate the UTS by up to -44%. The error coming from the simplified true stress evaluation demonstrates how the hypothesis that the section variation is inversely proportional to the longitudinal strain (equivalent to the 'constant volume' hypothesis for small deformations) does not hold: this is not surprising because in the literature, both analytical and experimental demonstrations of the soft tissue volume variation during tensile tests can be found [26,27]).

All sample properties are shown to be normally distributed, according to the Lilliefors test ($p<0.05$), so the following variance analysis could be performed.

The results of the analysis of variance are shown in Table 1: the type of treatment, its duration, and the specimen orientation are all significant factors, as is their interaction ($p<0.05$), with the

only exception of the specimen orientation for the ultimate strain. The mechanical behaviour along the CC direction is significantly stiffer compared to that in the ML direction, and the mechanical strength is higher (+77.1% E_e, +46.6% UTS_e, -16.1% $\varepsilon_{UTS,e}$, figures 3-5). DMEM treatment is generally less aggressive than NaOH treatment (figures 3-5), and the mechanical properties do not vary monotonously over the treatment length (figures 3-5).

A more detailed statistical analysis has been undertaken to establish which factor levels produced significantly different results compared to reference groups (respectively, T0-CC and T0-ML) by means of Tukey-Kramer tests, aiming to identify the best treatment type and duration as the combination producing the results most similar to those of native tissue. Looking at Figures 3-5, only minor differences exist between the engineering and 'simplified true' formulation results, and some general conclusions could be drawn. The tissue properties along the CC direction significantly degrade (lower UTS and E) for all treatments and durations, with $\varepsilon_{UTS,e}$ being the only mechanical property that is not affected significantly. In the ML direction, T0, DMEM T5, DMEM T6, DMEM T7, and NaOH T5 produce similar mechanical properties, according to both the engineering and simplified true formulations. These same treatments have been further investigated to assess if the true stress formulation would lead to the same conclusions. DMEM T5, DMEM T5, NaOH T5, and, partly NaOH T6 (assuming p=0.03) still produced mechanical properties close to those of native tissue for samples cut along the ML direction.

Native specimens cut along the CC direction continued to show a higher Young's modulus E_t and UTS_t; no treatment for any duration could preserve these properties.

4 Discussion

The native skin from which the HADM scaffold is prepared must be mechanically or physically separated from unwanted tissue and cell structures, and this processing step could alter the integrity and the architecture of the matrix and, in turn, influence the mechanical and material properties of the matrix. The efficiency of cell removal from a tissue is dependent on the origin of the tissue and the specific physical, chemical, and enzymatic methods that are used [28]. A similar consideration holds for the mechanical properties of the scaffold, as demonstrated in this work.

Experimental tests were performed at 20 °C, so the measured properties cannot be immediately converted to physiological properties at 37°C. The reason for this choice is the simplification of the experimental set up and being able to compare these results with most works in the literature in which mechanical tests have been carried out at 'room temperature' [8,11,15,29,17,18,30]. The results of the experimental tests were compared, assuming a perfectly uniaxial loading condition and a uniform distribution of collagen fibres. This is a limit in the present experimental set up, as the specimen is rectangular and its contraction is not allowed at the machine clamps, so the uniaxial stress hypothesis is not verified at the specimen ends. Using dog-bone shaped specimens would not completely solve this issue: in the case of longitudinal samples with most collagen fibres oriented axially, it would make no difference because the interrupted fibres (those placed more laterally) would be inactive. Longer specimens would have minimised the influence of the clamped ends, but they would have limited the maximum strain because the employed loading machine allows 12 mm displacement at the most. Finally, it should be stressed that the notch sensitivity in soft tissues is very low [23], so a minor area on the specimen is likely to be affected by the clamps. Ongoing numerical tests are confirming these hypotheses (nonlinear analysis, with large displacements, fig. 6), but the full strain field should be experimentally acquired as a final

validation. This is a quite demanding experimental set-up. Some authors are setting up systems based on digital image correlation [22]; this is certainly a promising technique that deserves to be considered in future tests on biological tissues.

Results have been here expressed through engineering, simplified true and true curves because the results of rupture tests for soft tissues have not always been reported in a standard manner in the literature [18]. Dealing with comparisons among different treatment types and durations and sample directions, all three representations produced substantially similar results.

A review of decellularization methods [6] agrees with the results here obtained regarding the NaOH cell removal treatment. In fact, it stated that bases are harsh, so are commonly used to eliminate growth factors from the matrix, even though they decrease ECM mechanical properties more significantly than chemical and enzymatic agents. In this work, the NaOH treatment has been proven to weaken the mechanical properties of the tissue, especially with reference to the cranio-caudal direction. The primary mechanism by which bases such as sodium hydroxide reduce the mechanical properties is the cleavage of collagen fibrils and disruption of collagen crosslinks. Richters *et al.* [31] evaluated a cost-effective method based on low concentrations of NaOH for the decellularization of human donor skin preserved in 85% glycerol, and they found that a 6 week incubation period was optimal, as stated in the present work, while longer periods caused damage to the collagen fibres, although the elastin fibres appeared to be well preserved, and this could explain the different behaviours observed along the cranio-caudal and medio-lateral directions.

DMEM coupled to mechanical action has been used as a cell removal treatment for the first time in this work, so similar tests cannot be found in the literature. Other decellularization methods include a wide variety of chemicals, but if the chemicals remain within the tissue in high concentrations after treatment, they can potentially invoke an adverse immune response by the

host (see, for example, enzymes commonly derived from bovine sources such as DNase, RNase, and trypsin). Herein, one of the most simple decellularization methods was studied (long-term incubation in culture medium), and preliminary immunohistochemical and histological results (unpublished data) demonstrate the complete decellularization of the tissue. DMEM treatment has also proven to be more conservative with reference to the medio-lateral direction because the mechanical properties of specimens treated with DMEM are generally higher than those measured on specimens treated with NaOH for the same number of weeks.

From a biological point of view, both DMEM and NaOH show, in the immunohistochemical evaluation, a good decellularization of grafts after only 4 weeks of treatment. However, the DMEM-treated samples exhibit better handling, greater flexibility and lower needle penetration resistance, according to surgeons' evaluations, and are therefore preferable. Additionally, the DMEM treatment avoids the use of chemical agents, as opposed to NaOH, which needs to be neutralized at the end of the decellularization process. Therefore, DMEM is less likely to produce inflammatory responses.

The objective of this work was to set up a procedure to perform biomechanical comparisons among decellularization treatments; the complete quantification of the skin's anisotropic behaviour would require a greater number of samples, from different donors, and biaxial testing. This experimental set up can allow only the measurement of the Young's modulus and failure properties along two reference orthogonal directions (parallel and perpendicular to the Langer's lines [8]). Nevertheless, in the following, a comparison with results obtained from other authors [8,32,33] is reported to verify the differences that exist and how they can be justified (Table 2).

Nì Annaidh *et al.* [8] reported force–displacement curves for each tensile test performed and calculated the engineering stress and strain. Their standard deviations were much larger; the

341 average coefficients of variation (ratios of the standard deviation to the mean) are up to 0.80 for
342 UTS and 0.97 for E, against the values obtained in this work, 0.09 and 0.10, respectively, due to
343 the number of specimens and the specimens having been taken from several donors (Table 2).
344 The values calculated in this work are most similar to those obtained on the 'lower back' and are
345 generally lower (up to -43% for UTS, up to -46% for ε_{UTS}, up to -68% for E) compared to those
346 reported in [8]. This can be explained by the smaller size of the specimens, which results in more
347 severe striction and consequently lower nominal stresses.
348 Yoder and Elliott [32] characterized human allografts by considering the engineering stress and
349 calculated two-dimensional Langrangian strains from optical images using Vic2D software. The
350 Young's modulus (Table 2) compares favourably to the results here reported for DMEM and
351 NaOH at T5 or T6 for engineering curves with reference to the ML direction. A 20 times higher
352 E along the 'parallel' direction is reported in [32]; this result is against the findings of this work
353 and [8], which both report a lower level of anisotropy in tested tissues.
354 Up to now, the failure properties and the elastic behaviour for static loads has been investigated,
355 as critical aspects of dermal patches include stiffness mismatch [35] and the eventual failure.
356 Nevertheless, cyclic loading parameters also need to be considered because in a highly
357 collagenous tissue such as skin, the elastic recoil and hysteresis of the material would be of utmost
358 importance.

359 # References

360

361 [1] Sander EA, Lynch KA, Boyce ST. Development of the mechanical properties of engineered
362 skin substitutes after grafting to full-thickness wounds. J Biomech Eng 2014;136:051008.
363 doi:10.1115/1.4026290.
364

[2] Sun BK, Siprashvili Z, Khavari PA. Advances in skin grafting and treatment of cutaneous wounds. Science 2014;346:941–5. doi:10.1126/science.1253836.

[3] Wong DJ, Chang HY. Skin tissue engineering. Harvard Stem Cell Institute; 2009.

[4] Badylak SF, Freytes DO, Gilbert TW. Reprint of: Extracellular matrix as a biological scaffold material: Structure and function. Acta Biomater 2015;23:S17–26. doi:10.1016/j.actbio.2015.07.016.

[5] Deeken CR, Eliason BJ, Pichert MD, Grant SA, Frisella MM, Matthews BD. Differentiation of biologic scaffold materials through physicomechanical, thermal, and enzymatic degradation techniques. Ann Surg 2012;255:595–604. doi:10.1097/SLA.0b013e3182445341.

[6] Crapo PM, Gilbert TW, Badylak SF. An overview of tissue and whole organ decellularization processes. Biomaterials 2011;32:3233–43. doi:10.1016/j.biomaterials.2011.01.057.

[7] Butler DL, Goldstein SA, Guilak F. Functional tissue engineering: the role of biomechanics. J Biomech Eng 2000;122:570–5.

[8] Ní Annaidh A, Bruyère K, Destrade M, Gilchrist MD, Otténio M. Characterization of the anisotropic mechanical properties of excised human skin. J Mech Behav Biomed Mater 2012;5:139–48. doi:10.1016/j.jmbbm.2011.08.016.

[9] Moore MA, Samsell B, Wallis G, Triplett S, Chen S, Jones AL, et al. Decellularization of human dermis using non-denaturing anionic detergent and endonuclease: a review. Cell Tissue Bank 2015;16:249–59. doi:10.1007/s10561-014-9467-4.

[10] Eshel H, Lanir Y. Effects of strain level and proteoglycan depletion on preconditioning and viscoelastic responses of rat dorsal skin. Ann Biomed Eng 2001;29:164–72.

[11] Sanders R. Torsional elasticity of human skin in vivo. Pflugers Arch 1973;342:255–60.

[12] Fung YC. Biomechanics - Mechanical Properties of Living Tissues | Y. C. Fung | Springer. 2nd ed. New York: Springer-Verlag; 1993.

[13] Pereira BP, Lucas PW, Swee-Hin T. Ranking the fracture toughness of thin mammalian

403 soft tissues using the scissors cutting test. J Biomech 1997;30:91–4.
404

405 [14] Del Prete Z, Antoniucci S, Hoffman AH, Grigg P. Viscoelastic properties of skin in Mov-
406 13 and Tsk mice. J Biomech 2004;37:1491–7. doi:10.1016/j.jbiomech.2004.01.015.
407

408 [15] Muñoz MJ, Bea J a., Rodríguez JF, Ochoa I, Grasa J, Pérez del Palomar a., et al. An
409 experimental study of the mouse skin behaviour: Damage and inelastic aspects. J Biomech
410 2008;41:93–9. doi:10.1016/j.jbiomech.2007.07.013.
411

412 [16] Liu Z, Yeung K. On Preconditioning and Stress Relaxation Behaviour of Fresh Swine Skin
413 in Different Fibre Direction. Biomed Pharm Eng 2006 ICBPE 2006 Int Conf 2006:221–6.
414

415 [17] Jacquemoud C, Bruyere-Garnier K, Coret M. Methodology to determine failure
416 characteristics of planar soft tissues using a dynamic tensile test. J Biomech 2007;40:468–
417 75. doi:10.1016/j.jbiomech.2005.12.010.
418

419 [18] Khanafer K, Schlicht MS, Berguer R. How Should We Measure and Report Elasticity in
420 Aortic Tissue? Eur J Vasc Endovasc Surg 2013;45:332–9. doi:10.1016/j.ejvs.2012.12.015.
421

422 [19] Euro Tissue Bank - Manual n.d. http://www.eurotissuebank.nl/euro-skin-bank-huidbank-
423 esb-en-GB/what-is-donor-skin/manual/ (accessed October 14, 2015).
424

425 [20] Arumugam V, Naresh MD, Sanjeevi R. Effect of strain rate on the fracture behaviour of
426 skin. J Biosci 1994;19:307–13. doi:10.1007/BF02716820.
427

428 [21] Hosseini SM, Wilson W, Ito K, van Donkelaar CC. How preconditioning affects the
429 measurement of poro-viscoelastic mechanical properties in biological tissues. Biomech
430 Model Mechanobiol 2013:503–13. doi:10.1007/s10237-013-0511-2.
431

432 [22] Bel-Brunon A, Kehl S, Martin C, Uhlig S, Wall WA. Numerical identification method for
433 the non-linear viscoelastic compressible behavior of soft tissue using uniaxial tensile tests
434 and image registration - application to rat lung parenchyma. J Mech Behav Biomed Mater
435 2014;29:360–74. doi:10.1016/j.jmbbm.2013.09.018.
436

437 [23] Taylor D, O'Mara N, Ryan E, Takaza M, Simms C. The fracture toughness of soft tissues.
438 J Mech Behav Biomed Mater 2012;6:139–47. doi:10.1016/j.jmbbm.2011.09.018.
439

440 [24] Özkaya N, Nordin M, Goldsheyder D, Leger D. Fundamentals of Biomechanics -

Equilibrium, Motion, and | Nihat Özkaya | Springer. 3rd ed. New York: Springer-Verlag; 2012.

[25] Silver FH, Freeman JW, DeVore D. Viscoelastic properties of human skin and processed dermis. Skin Res Technol 2001;7:18–23.

[26] Adeeb S, Ali A, Shrive N, Frank C, Smith D. Modelling the Behaviour of Ligaments: A Technical Note. Comput Methods Biomech Biomed Engin 2004;7:33–42. doi:10.1080/10255840310001637266.

[27] Reese SP, Maas SA, Weiss JA. Micromechanical models of helical superstructures in ligament and tendon fibers predict large Poisson's ratios. J Biomech 2010;43:1394–400. doi:10.1016/j.jbiomech.2010.01.004.

[28] Chen R-N, Ho H-O, Tsai Y-T, Sheu M-T. Process development of an acellular dermal matrix (ADM) for biomedical applications. Biomaterials 2004;25:2679–86. doi:10.1016/j.biomaterials.2003.09.070.

[29] Li L, Qian X, Wang H, Hua L, Zhang H, Liu Z. Power type strain energy function model and prediction of the anisotropic mechanical properties of skin using uniaxial extension data. Med Biol Eng Comput 2013;51:1147–56. doi:10.1007/s11517-013-1098-6.

[30] Ní Annaidh A, Bruyère K, Destrade M, Gilchrist MD, Maurini C, Otténio M, et al. Automated Estimation of Collagen Fibre Dispersion in the Dermis and its Contribution to the Anisotropic Behaviour of Skin. Ann Biomed Eng 2012;40:1666–78. doi:10.1007/s10439-012-0542-3.

[31] Richters CD, Pirayesh A, Hoeksema H, Kamperdijk EWA, Kreis RW, Dutrieux RP, et al. Development of a dermal matrix from glycerol preserved allogeneic skin. Cell Tissue Bank 2008;9:309–15. doi:10.1007/s10561-008-9073-4.

[32] Yoder JH, Elliott DM. Nonlinear and anisotropic tensile properties of graft materials used in soft tissue applications. Clin Biomech 2010;25:378–82. doi:10.1016/j.clinbiomech.2010.01.004.

[33] Edwards C, Marks R. Evaluation of biomechanical properties of human skin. Clin Dermatol 1995;13:375–80. doi:10.1016/0738-081X(95)00078-T.

[34] Daly CH. Biomechanical properties of dermis. J Invest Dermatol 1982;79 Suppl 1:17s –

20s.

[35] Hopp I, Michelmore A, Smith LE, Robinson DE, Bachhuka A, Mierczynska A, et al. The influence of substrate stiffness gradients on primary human dermal fibroblasts. Biomaterials 2013;34:5070–7. doi:10.1016/j.biomaterials.2013.03.075.

488

489 ***Table 1: Anova results for the ultimate stress, ultimate strain and elastic modulus with reference to***
490 ***the engineering formulation. Boldface characters are used to highlight factors that are not significant***
491 ***(p > 0.05)."***
492

Ultimate Stress					
Source	**Sum Sq.**	**DOF**	**Mean Sq.**	**F**	**p**
Treatment	30.90	1	30.90	128.22	6.28E-17
Orientation	11.00	1	11.00	45.67	4.94E-09
Duration	257.24	7	36.75	152.50	2.08E-37
Treatment*Orientation	12.04	1	12.04	49.97	1.41E-09
Treatment*Duration	13.57	7	1.94	8.05	5.45E-07
Orientation*Duration	64.42	7	9.20	38.19	1.67E-20
Error	15.42	64	0.24		
Total	421.99	95			

Ultimate Strain					
Source	**Sum Sq.**	**DOF**	**Mean Sq.**	**F**	**p**
Treatment	0.37	1	0.37	40.22	2.61E-08
Orientation	0.00	1	0.00	0.27	**6.05E-01**
Duration	0.45	7	0.07	7.00	3.42E-06
Treatment*Orientation	0.06	1	0.06	6.73	1.17E-02
Treatment*Duration	0.76	7	0.11	11.80	1.52E-09
Orientation*Duration	0.44	7	0.06	6.86	4.40E-06
Error	0.59	64	0.01		
Total	2.94	95			

Elastic Modulus					

Source	Sum Sq.	DOF	Mean Sq.	F	p
Treatment	318.03	1	318.03	108.72	1.98E-15
Orientation	98.80	1	98.80	33.77	2.13E-07
Duration	748.22	7	106.89	36.54	5.10E-20
Treatment*Orientation	44.72	1	44.72	15.29	2.25E-04
Treatment*Duration	295.62	7	42.23	14.44	4.16E-11
Orientation*Duration	578.59	7	82.66	28.26	2.67E-17
Error	187.22	64	2.93		
Total	2386.48	95			

497

498

499 ***Table 2 Mechanical properties of skin in literature and in this work (average± SD).***

Author	Skin Location (Langer Line Orientation)	UTS (MPa)	Failure Stretch	Elastic Modulus (MPa)	Reference Variables
Nì Annaidh *et al.* [8]	Middle Back (Parallel)	28.64 ± 9.03	1.46 ± 0.07	112.47 ± 36	σ_e,ε_e
	Bottom Back (Parallel)	17.60 ± 4.77	1.74 ± 0.32	73.81 ± 19.41	
	Middle Back (Perpendicular)	16.53 ± 5.71	1.52 ± 0.08	63.75 ± 24.59	
	Bottom Back (Perpendicular)	10.56 ± 8.41	1.61 ± 0.14	37.66 ± 36.41	
Edwards C. [33]		5-30	35-115%	15-150	Various authors
Yoder and Elliott [32]	Alloderm (Parallel)			221.48 ± 141.20	σ_e,$\varepsilon_{Lagrange}$
	Alloderm (Perpendicular)			11.21 ± 3.53	
This work (T_0)	Back (craniocaudal)	10.28 ± 0.96	0.77 ± 0.08	13.01 ± 2.61	σ_e,ε_e,E_e
		18.38 ± 2.42			σ_{st}
		33.95 ± 4.93		43.63 ± 6.29	σ_t, E_t
	Back (medio-lateral)	7.01 ± 0.10	0.93 ± 0.15	7.20 ± 1.22	σ_e,ε_e,E_e
		13.81 ± 2.80			σ_{st}
		24.11 ± 3.24		29.77 ± 7.54	σ_t, E_t

500

Figure Captions

Figure 1. (Left) An interpolated engineering stress-strain curve, its descriptive parameters, and specimen images. (Right) Experimental stress strain curves, where point 'U' represents the average ultimate strain/stress point with its standard deviations; a) DMEM, T6, ML direction; b) DMEM, T6, CC direction; c) NaOH, T6, ML direction; d) NaOH, T6, CC direction.

Figure 2. Engineering, simplified true, and true formulation curves; a) DMEM, T6, ML direction; b) DMEM, T6, CC direction; c) NaOH, T6, ML direction; d) NaOH, T6, CC direction"

Figure 3. UTS values obtained from engineering, simplified true, and true formulations for different decellularization treatments. Left side (grey background): results obtained along CC direction; right side (white background): results obtained along ML direction

Figure 4. Engineering strain corresponding to the ultimate stress for different decellularization treatments. Left side (grey background): results obtained along CC direction; right side (white background): results obtained along ML direction

Figure 5. Elastic modulus values for different decellularization treatments. Left side (grey background): results obtained along CC direction; right side (white background): results obtained along ML direction

Figure 6. Axial stress distribution from finite element analysis: nonlinear 3D analysis (Ansys Mechanical APDL); hexahedral mesh of 600 elements (SOLID186); E=14 MPa; Poisson's ratio = 0.4; all displacements have been constrained at the lower edge, while the upper edge can only move vertically, where u=2 mm (ε=0.4) has been applied

Figure 1

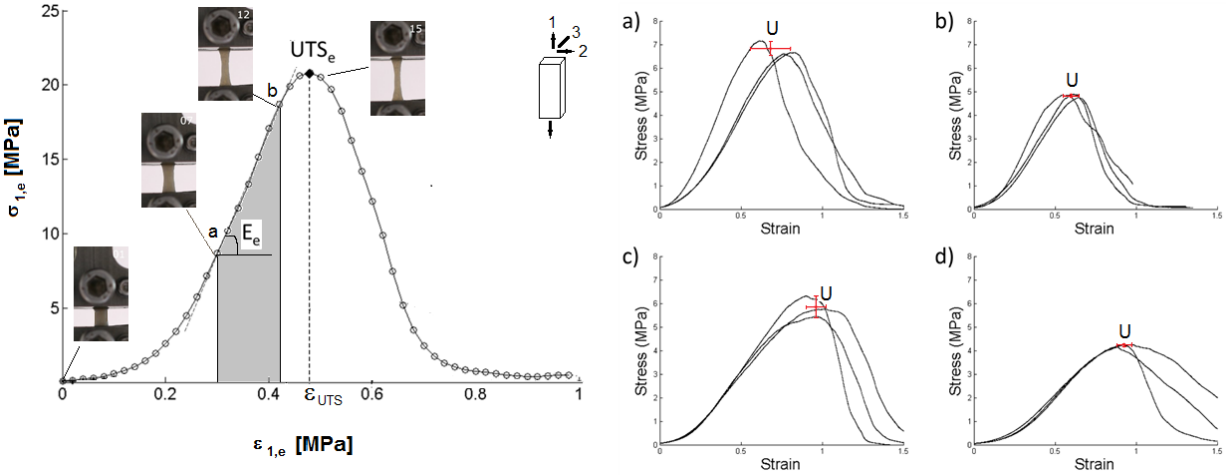

Figure 2

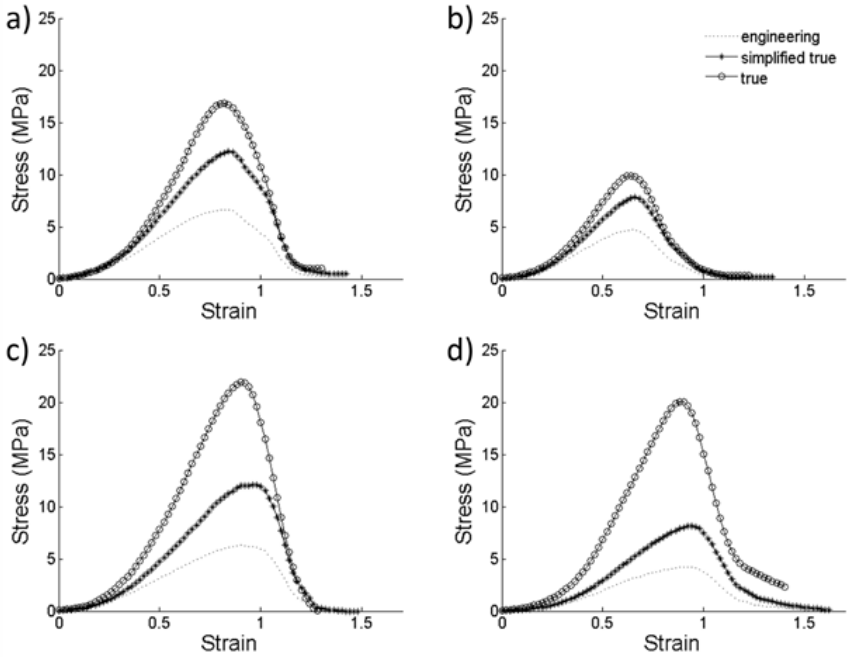

Figure 3

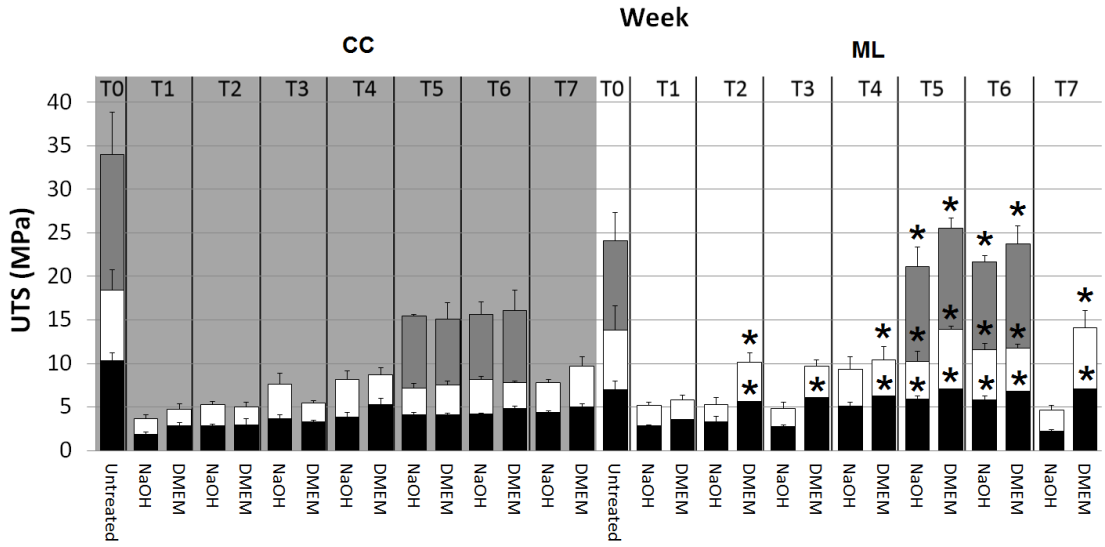

Figure 4

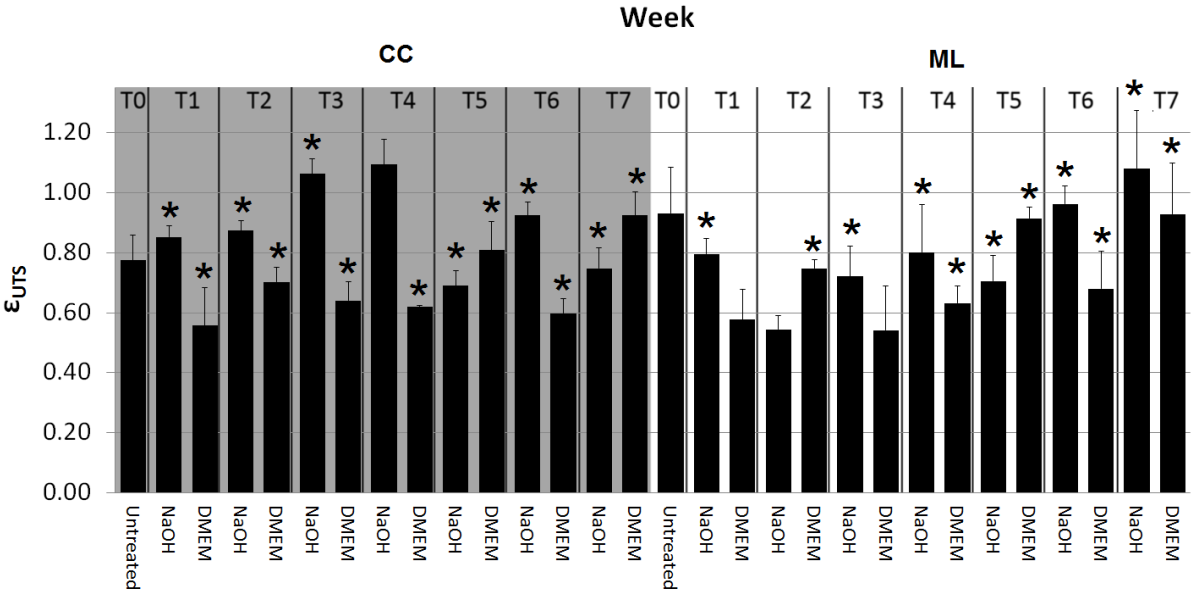

533 **Figure 5**

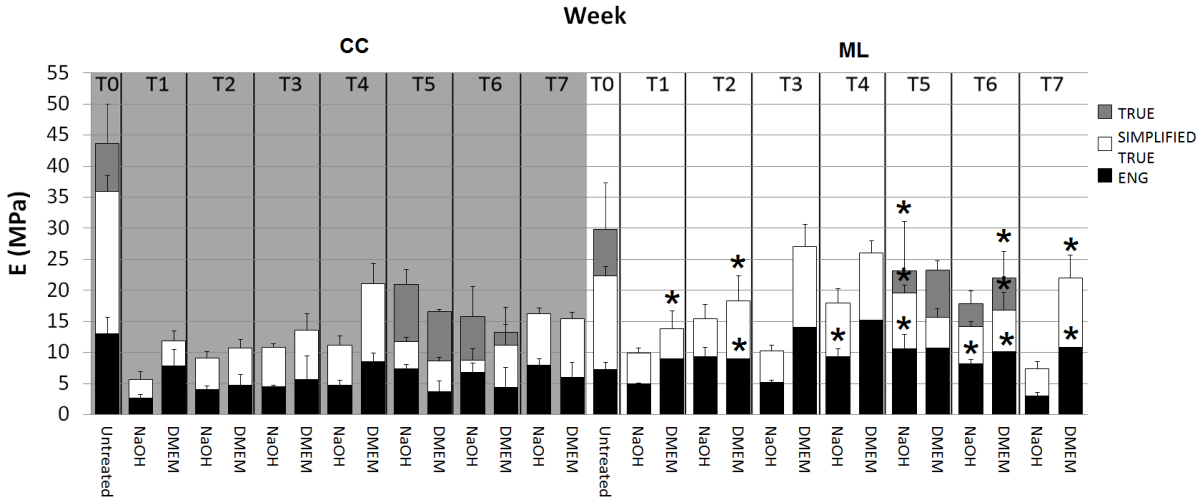

534

535 **Figure 6**

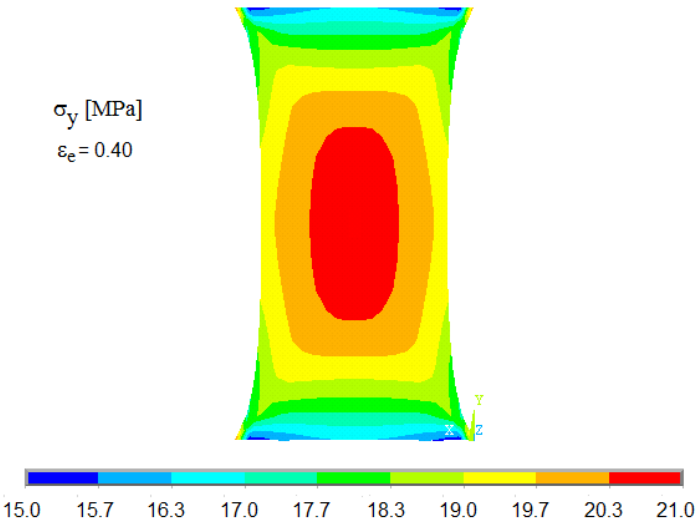

536